Supporting Information

Photoactive PDI-Cobalt Complex immobilized on Reduced Graphene Oxide for Photoelectrochemical Water Splitting.

Janardhan Balapanuru,[a,b] Gordon Chiu,[b] Chenliang Su, [a] Na Zhou,[a] Zhu Hai,[a] Xu Qinghua,[a] and Kian Ping Loh[a]*

* Corresponding author's email: chmlohkp@nus.edu.sg

[a] Department of Chemistry and Graphene Research Centre (GRC) ,

   National University of Singapore, 3 Science Drive 3, Singapore 117543.

[b] Graphite Zero Pte. Ltd., 20 Maxwell Road, #11-18,

   Maxwell House, Singapore 069113.

Contents

S1. Materials and Methods

   S1.1. Synthesis of Graphene Oxide (GO)

   S1.2. Synthesis of reduced Graphene Oxide (rGO)

   S1.3. Synthesis of Perylene tetracarboxylic Di-(propyl Imidazole) (PDI)

   S1.4. Bandgap calculations

   S1.5. Synthesis of Co-ordination polymer [PDI-Co-Cl2(H2O)2]n or PDI-Co

   S1.6. Synthesis of rGO-PDI-Co

S1.7. Preparation of electrodes and Photoelectrochemical measurements

Figure S1. Scanning electron microscopic (SEM) images of PDI.

Figure S2: Frontier orbitals of PDI calculated using DFT at the B3LYP/6-31G*

Figure S3. Comparative FITR Spectra of PDI, PDI-Co, rGO and rGO-PDI-Co

Figure S4: Scanning Electron Microscopy (SEM) , Electron Dispersion X-ray spectroscopy (EDS) analysis of **PDI-Co**

Figure S5: SEM images of PDI-Co and rGO-PDI-Co complex.

Figure S6: Thermo gravimetric analysis (TGA) recorded in N_2 atmosphere at scan rate of 10°C/min (a) comparative analysis (b) PDI-Co (b) rGO and (c) rGO-PDI-Co complex.

Estimation of active Cobalt concentration in rGO:PDI-Co (ratio 0.4:1)

Calculation of turnover number (TON vs Co^{II})

Charge-transfer Pump-Probe experiments

Catalyst Stability- Recycle test

APPENDIX-I

S1. Materials and Methods

Chemicals and Materials: $CoCl_2.6H_2O$ was purchased from Alfa Asear All other chemicals were purchased from Sigma Alrdrich and used without further purification, including Perylene-3,4,9,10-tetracarboxylic dianhydride, Imidazole, sodium borohydride (~ 98%). All solvents were reagent grade and purified before use.

S1.1. Synthesis of Graphene Oxide (GO) [1]

Under constant stirring, 3 g of MesoGraf^{TM} powder (obtained from Graphite Zero Pte. Ltd., Singapore) and 9 g of $KMnO_4$ was added to a 9:1 mixture of Conc. H_2SO_4/H_3PO_4 (180:20 mL). The reaction mixture was stirred at room temperature for 12 h and 30% H_2O_2 (3 mL) was slowly added to the reaction mixture to stop the reaction. Later, it was washed with DI water *via* centrifugation till the pH reaches to 4-5.

S1.2. Synthesis of reduced Graphene Oxide (rGO)

400 mg of dried GO was placed in a quartz tube and annealed at 300°C under hydrogen atmosphere. Most of the oxygen functional groups were removed to get conductive reduced graphene oxide (rGO) sheets.

S1.3. Synthesis of Perylene tetracarboxylic Di-(propyl Imidazole) (PDI):
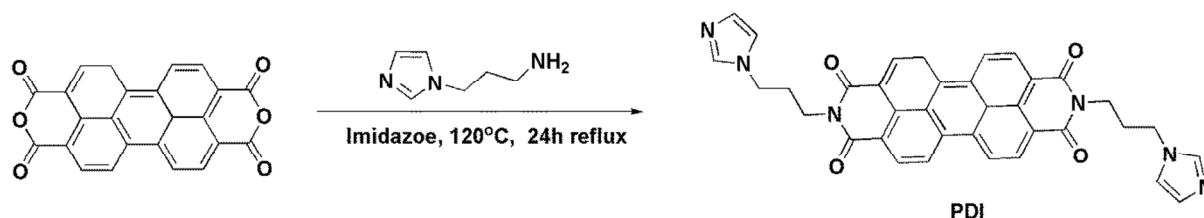
In an inert atmosphere, 15 g of imidazole and Perylene-3,4,9,10-tetracarboxylic dianhydride (2 g, 1.27 mmol) was mixed with 4 mL of 1-(3-aminopropyl) imidazole and heated to 120°C for 12 h. The reaction mixture was cooled to room temperature and the crude solid was dissolved in 250 mL of $CHCl_3$ and sonicated for 30 min. 300 mL of DI water was added to $CHCl_3$ solution and the unreacted anhydride precipitate was separated by filtration. The remaining compound in $CHCl_3$ solution was further washed with DI water for several times to

remove dissolved imidazole. Finally, the fluorescent compound Perylene tetracarboxylic Di-(propylimidazole) (**PDI**) (500 mg, 25% yield) was obtained after evaporating $CHCl_3$. Molecular formula of PDI: $C_{36}H_{28}N_6O_4$, MALDI- TOF (+m/z) 607; (-m/z) 606. Elemental Analysis: C % 71.04, H% 4.64, N% 13.81. The product can be grown into microcrystalline wires of size >10 μm (**Fig. S1**).
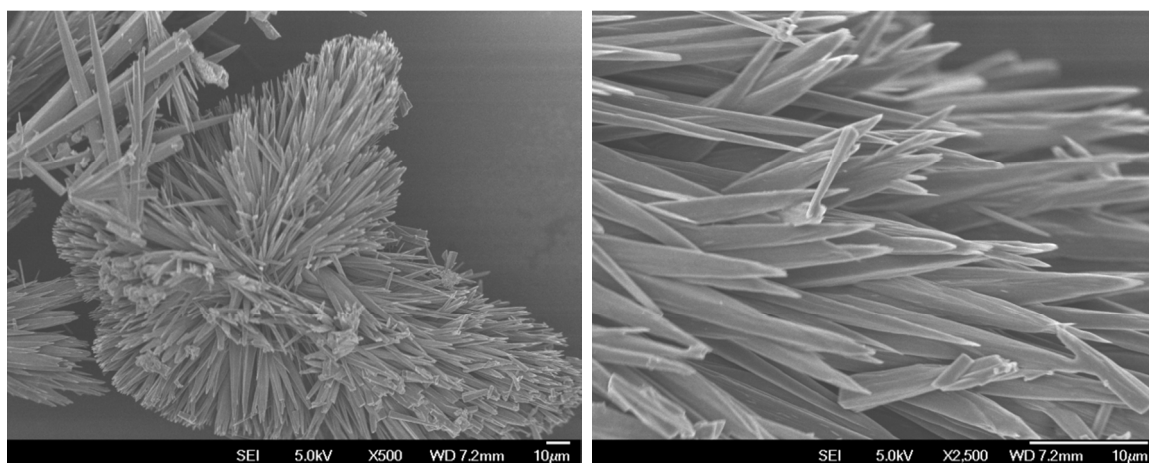
Figure S1. Scanning electron microscopic (SEM) images of PDI. Higher magnification (right)

S1.4. Band gap calculations:

The geometry optimizaion of PDI was performed using Gaussian 09 at the density functional theory (DFT) level with the B3LYP functional and a 6-31G* basis set.

4

HOMO   **LUMO**
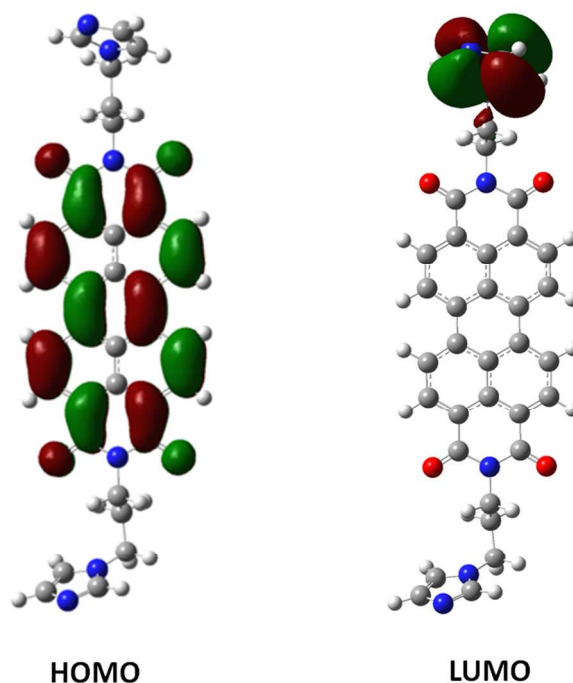
Figure S2: Frontier orbitals of PDI calculated using DFT at the B3LYP/6-31G*

The HOMO and LUMO surfaces are generated from the optimized geometries using GaussView 5. The calculated HOMO and LUMO levels for PDI are at **-6.006 eV** and **-3.699 eV** which are consistent with previously reported perylene derivatives.[2]

S1.5. Synthesis of Co-ordination polymer [PDI-Co-Cl₂(H2O)₂]ₙ or PDI-Co:

As shown in the **Fig. 1(a) (main text),** a very dilute 15 mL solution of PDI in CHCl₃ was filled in a 20 mL glass vial and heated to 60°C slowly. Later, a 0.5mL ethanol solution of CoCl₂.6H₂O was added as a top layer on the PDI solution (**Fig. 1 (b)**) and heating was continued for 4 h. The color of the mixture turned pink and a crystalline product of **[PDI-Co-Cl₂(H2O)₂]ₙ or PDI-Co** (**Fig. 1(c)**) precipitated. The product was filtered and washed several times with ethanol to remove unreacted CoCl₂. 6H₂O.[3]

S1.6. Synthesis of rGO:PDI-Co: (0.4 :1.0)

40 mg of rGO was sonicated in 50 mL of dimethyl formamide (DMF) and 50 ml of PDI-Co (2 mg/mL) was added and stirred for overnight at 90°C. As obtained rGO-PDI-Co product was filtered and dried under vacuum conditions. The same method was adapted to prepare remaining rGO-PDI-Co composites.

S1.7. Preparation of electrodes and Photoelectrochemical measurements

20 mg of samples were dispersed in DMF/Ethanol (1:1, 5 mL) solution and drop casted on ITO (2 cm x 1 cm) plates which were later dried on a hot surface at 65°C for 10 min. Photoelectrochemical experiments were conducted using standard 3-electrode system where sample-coated ITO plates were used as working electrodes, Pt-wire as counter electrode and Ag/AgCl as reference electrode. The cell was controlled using a CH Instruments potentiostats (CHI 832 and CH 660D). Linear sweep voltammogram (LSV)s were recorded at scan speed of 10 mV s^{-1} under visible light irradiation (300W xenon lamp with a 400 nm cut-off filter as a visible light source.) Following, HER is quantified using a online gas chromatographic (GC) TCD detector. The evolution of hydrogen gases during the photoelectrochemical water splitting reaction is measured for all samples in 1 M PBS buffer solution at pH 6.8 with an applied bias of -0.4 V vs SHE.

**Fourier Transform Infrared Spectroscopy (FTIR) studies:**
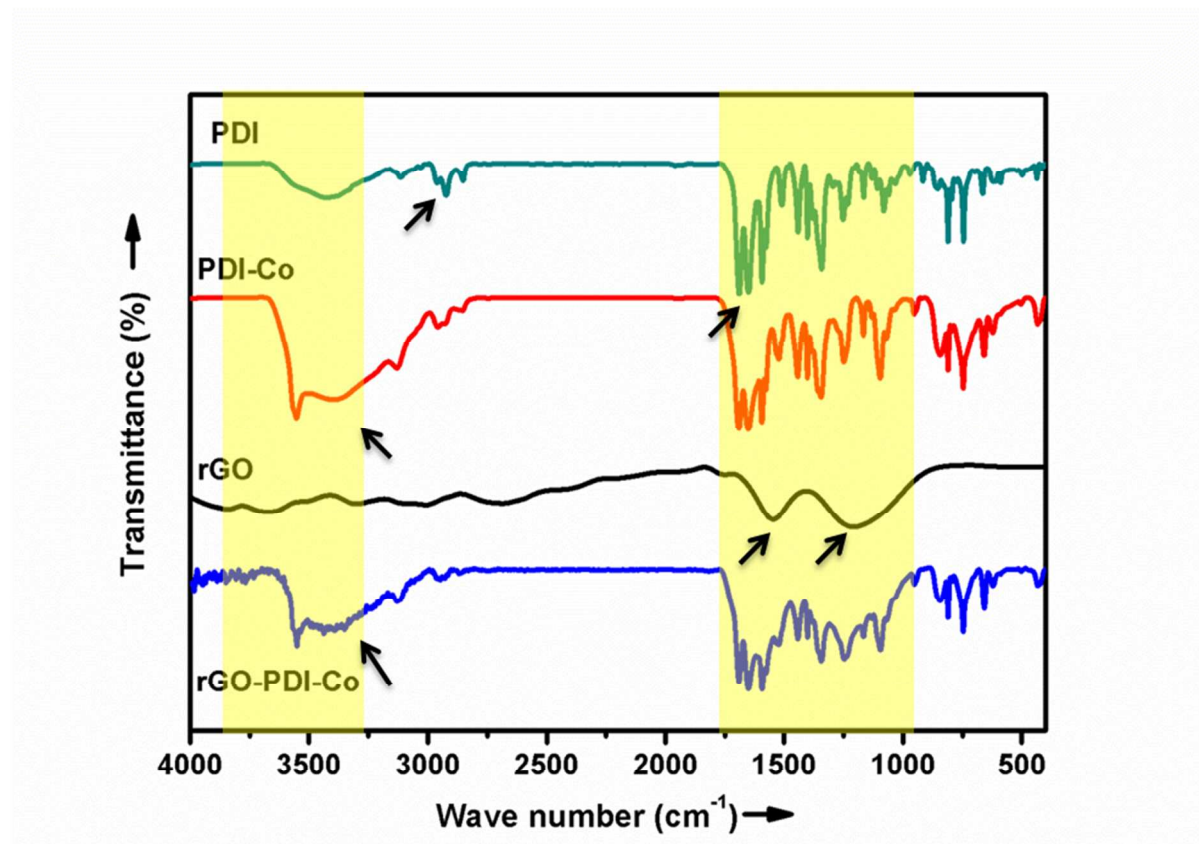
Figure S3. Comparative FITR Spectra of PDI, PDI-Co, rGO and rGO-PDI-Co

Fourier Transform Infrared (FITR) spectra of all the samples are presented above.   In **Fig. S3,** the presence of the imide linkage can be evidenced by the 1691 cm^{-1} and 1649 cm^{-1} peaks, which correspond to the *in-plane* (asymmetric) and *out of plane* (symmetric) –C=O stretching, respectively.[2] The peak at 1343 cm^{-1} is attributed to C-N-C absorption of the imide ring.[2] The peak at 2992 cm^{-1} is ascribed to the –C-H vibration from the methylene group of the spacer.[2] Broader and characteristic peaks at 3558 cm^{-1} and 3390 cm^{-1} for PDI-Co are mainly due the strong –OH stretching vibrations.[4] The –OH peak also can be seen in rGO-PDI-Co complex. In the case of rGO, there are two broad peaks at 1553cm^{-1} and 1288 cm^{-1} which are

attributed to residual –C-O functional groups.[4] For rGO-PDI-Co, the overlap of rGO and PDI-Co peaks between 800 cm^{-1} to 1600 cm^{-1} was observed.

**SEM and Energy-dispersive X-ray spectroscopy (EDS) Mapping:**
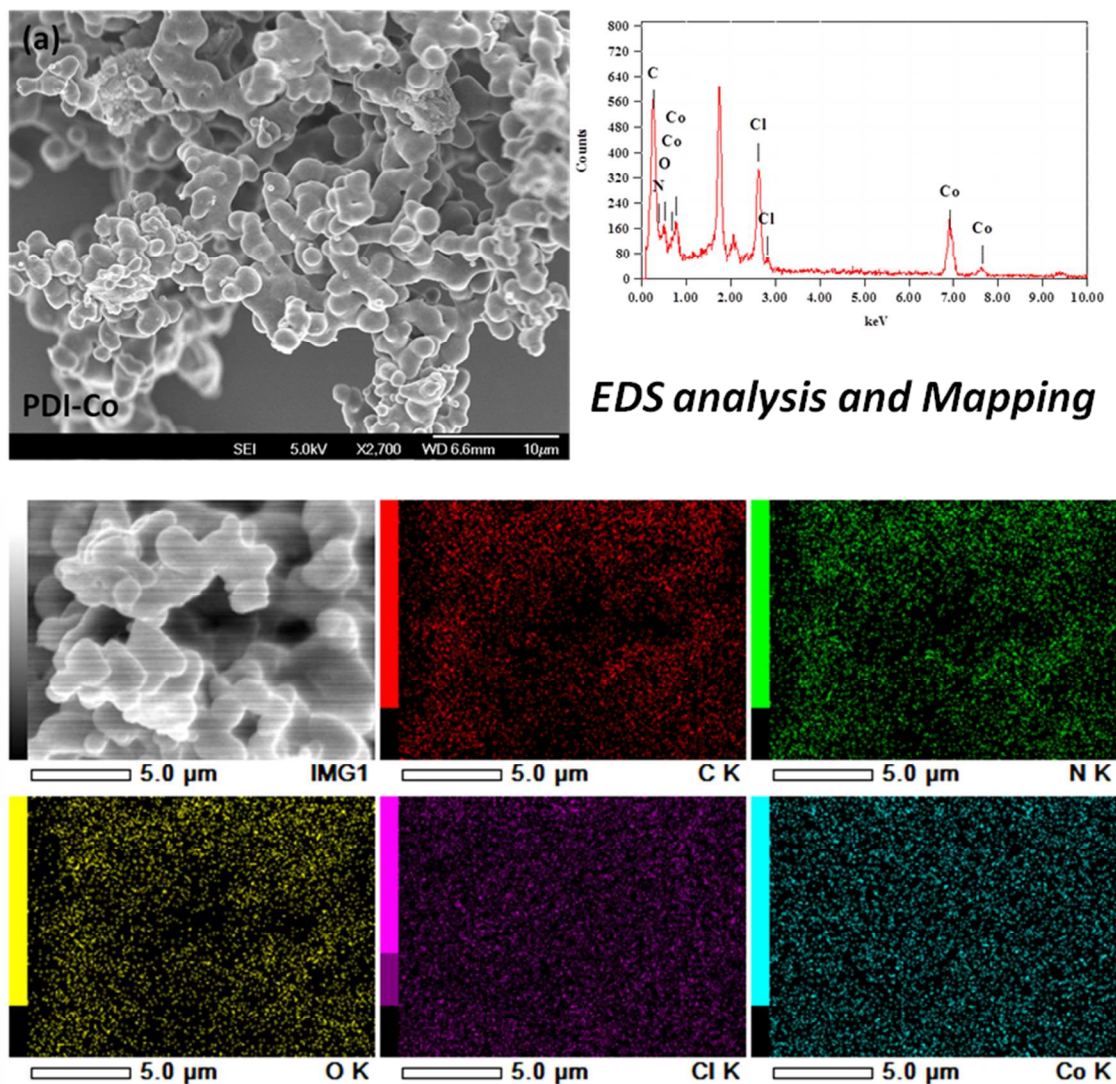
Figure S4: Scanning Electron Microscopy (SEM) , Electron Dispersion X-ray spectroscopy (EDS) analysis of **PDI-Co**

Scanning Electron Microscopy (SEM) and Electron Dispersion X-ray Spectroscopy (EDS) analysis of **PDI-Co** show the morphology and spatial distribution of C, N, O, Co and Cl

elements in the composite. (**Fig. S4**) From the EDS analysis, the characteristic Co and Cl peaks can been clearly seen at 2.2 keV and 7.2 keV respectively.[6] The morphology analysis shows that when rGO is introduced to PDI-Co to form rGO-PDI-Co, the PDI-Co particles are absorbed or wrapped on the rGO sheets. (**Fig. S5**) The surface interaction between rGO and PDI-Co enables a multichannel environment which facilitates efficient charge injection within the composite.[5]
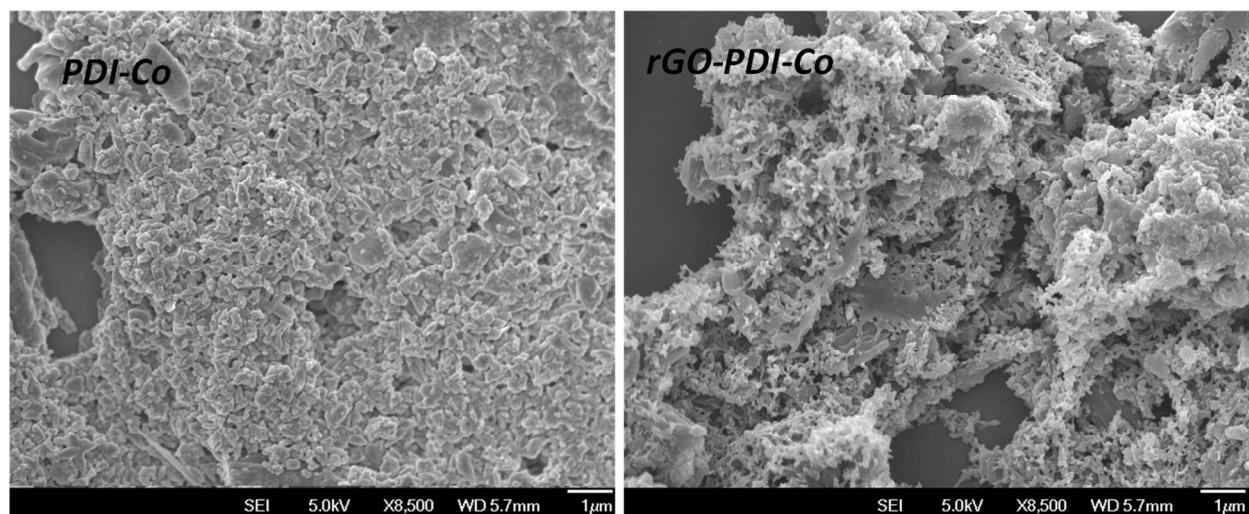

Figure S5: Scanning Electron Microscopy (SEM) images of PDI-Co and rGO-PDI-Co complex.

Thermogravimetric Analysis (TGA):

The thermal stability of PDI-Co, rGO and rGO-PDI-Co composites was investigated by thermal gravimetric analysis under N_2 atmosphere and with a heating ramp of 10°C/min to 800°C. In the case of PDI-Co, the major weight loss at ~100°C is mainly due to the H_2O molecules which are bound to the cobalt metal (**Fig. S6**). The weight losses at 320°C and 450°C are caused by the decomposition of oxygen and imidazole functional groups and the perylene core.[7] As shown in **Fig. S6(c)**, rGO is quite robust up to 600°C and decomposition above 600 °C may be due to oxidation by trace oxygen in the atmosphere to form volatile CO and CO_2 species.

[4] The rGO-PDI-Co shows a thermal decomposition profile that is weighted by the proportions of PDI-Co and rGO in the composite.
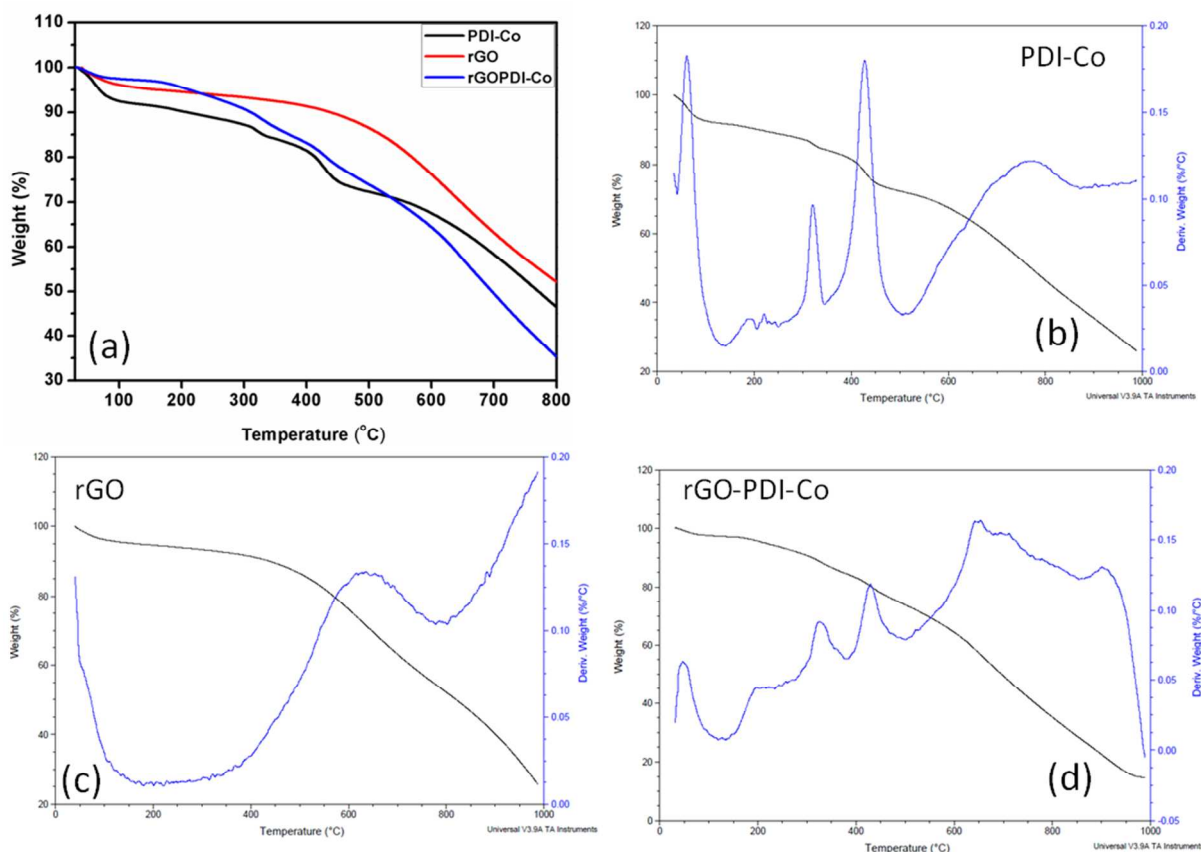
Figure S6: Thermo gravimetric analysis (TGA) recorded in N_2 atmosphere at scan rate of 10°C/min (a) comparative analysis (b) PDI-Co (b) rGO and (c) rGO-PDI-Co complex.

Estimation of active Cobalt concentration in rGO:PDI-Co (ratio 0.4:1):

Charge $Q = \frac{1}{v} \int_{Vo}^{Vf} I(V).dV$ ……………………………….(Eq. 1)

v is scan rate (10 mV.s^{-1}), I is current density (mA /cm^2) V_0 intial and V_f final voltages,   The integration represents the area under the curve at -1.04 V [Co(II)/Co(I)] and is obtained as 0.08389 mA.cm^{-2}.V (Calculated using Orgin 8.0 software) (**Fig. 3** main text)

Charge Q $= \frac{1}{10} \times 0.08389. \left(\frac{V.mA.cm^{-2}}{mV.s^{-1}} \right)$

Charge Q $= 0.008389$ A. s. cm^{-2} or Coulomb/cm^2

$Q = n_e \times F$ ....(Eq. 2)

Q= charge (C /cm^2), n_e= no. of electrons/mol, F = Faraday constant = 9.648× 10^4 C /mol

$$n_e = \frac{Q}{F} \left(\frac{C.cm^{-2}}{C.mol^{-1}} \right)$$

$$n_e = \frac{0.008389}{9.648 \times 10^4} \text{ mol. cm}^{-2}$$

Number of electrons (in terms of moles per cm^{-2}) $n_e = 7.21 \times 10^{-8}$ mol.cm^{-2}

Since, one mole of electrons are involved in one mole of Co(II)/Co(I) reduction,[7]

No. of moles of electrons/cm^2 = No. of moles of Cobalt active species/cm^2.

Hence, the amount of active cobalt [Co(II)/Co(I)] in rGO-PDI-Co = 7.21 × 10^{-8} mol.cm^{-2}

Calculation of turnover number (TON vs Co^{II}):

$Q = n_e \times F$ ....(Eq. 3)

Q is the charge (C /cm^2) developed during the photoelectrochemical hydrogen evolution process at rGO-PDI-Co i.e., 10.5 C/cm^2 (From **Fig. 6(b)** main text)

n_e is the number of electrons/mol and F is Faraday constant (9.648× 10^4 C /mol)

$$n_e = \frac{Q}{F} \left(\frac{C.cm^{-2}}{C.mol^{-1}} \right)$$

$$n_e = \frac{10.5}{9.648 \times 10^4} \text{ mol. cm}^{-2}$$

So, the total number of electrons (in terms of moles per cm^{-2}) = 1.088×10^{-4} mol.cm^{-2}

Since two electrons are required to generate one molecule of H$_2$,[7]

No. of moles of hydrogen generated = (no. of moles of electrons)/ 2

No. of moles of hydrogen generated = 1.088×10^{-4} mol.cm^{-2}/ 2

No. of moles of hydrogen generated = 0.544×10^{-4} mol.cm^{-2}

Turn over number $= \dfrac{no.\, of\; moles\; of\; H2\; generated}{no.\, of\; moles\; of\; active\; Cobalt\; species (estimated\; from\; CV\; curves\,)}$

$$= \frac{0.544 \times 10^{-4}\; mol.cm^{-2}}{7.21 \times 10^{-8}\; mol.cm^{-2}}$$

TON = 754 (after 5 hrs of operation).

Charge-transfer Pump-Probe experiments:

To investigate the charge transfer in the **PDI-Co** complex, femtosecond pump-probe experiments were carried out on DMF solutions of **PDI-Co, rGO** and **rGO-PDI-Co.** Laser pulses were generated from a mode-locked Ti:sapphire oscillator (Spectra Physics) seeded regenerative amplifier with a pulse energy of 2mJ at 800nm and a repetition rate of 1 kHz. The 800 nm laser beam was split in two, one branch passed through a BBO crystal to generate the 400 nm pump beam by frequency-doubling and another branch was used to generate a white light continuum in a 1mm sapphire plate. The white light continuum was again split into two beams, a probe and a reference. The signal and reference beams were detected by photodiodes that are connected to lock-in amplifiers and the computer. The intensity of the pump beam was attenuated with the

neutral density filter. The pump beam was focused onto the sample with a beam size of 300 μm and overlaps the smaller-diameter (100 μm) probe beam. The delay between pump and probe pulses was varied by a computer controlled translation stage. The pump beam was modulated by optical chopper at frequency of 500 Hz. The transient absorption spectra at different delay times were measured by passing the probe beam through monochromator before being detected by a photo diode that is connected to the lock-in amplifier. [10]

Catalyst Stability- Recycle test:
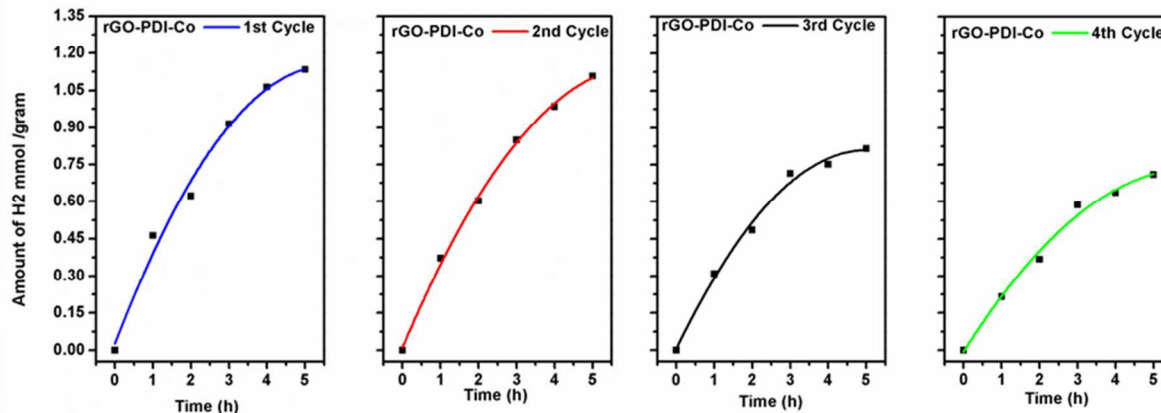
Figure S7: (a) Recycle-test of the rGO-PDI-Co electrode illuminated under visible light and at an applied potential of -0.4V (vs RHE) [0.1 M phosphate buffer, pH ~7.0, (5% Triethylamine (TEA) was used as hole scavenger)]
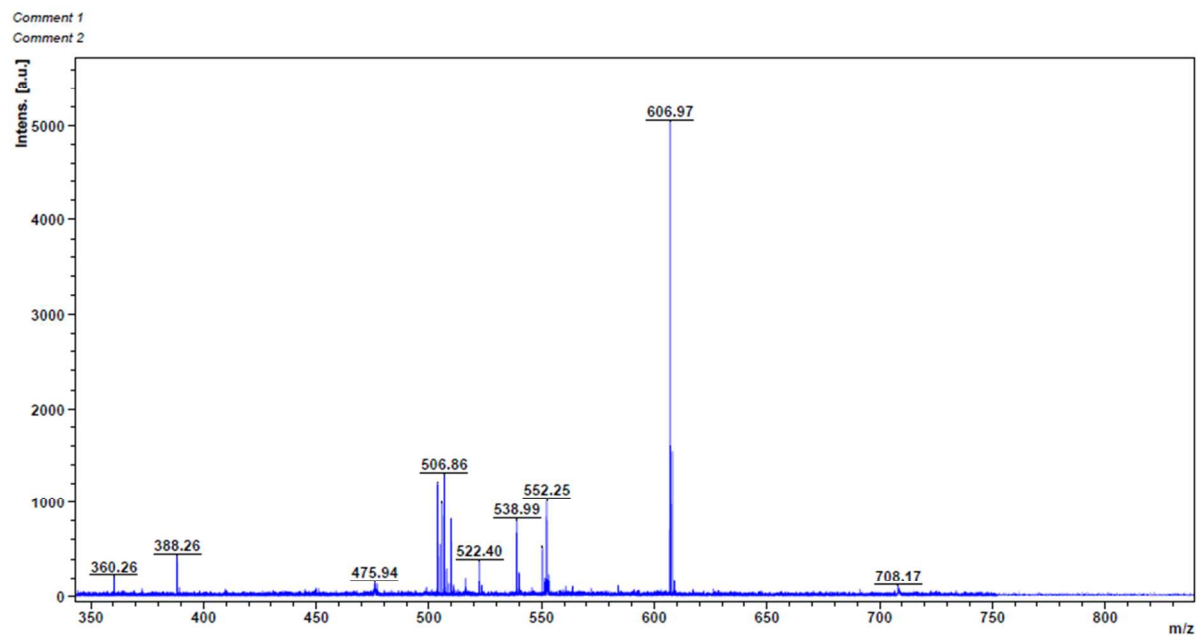
We have also investigated the reusability of rGO-PDI-Co in multiple testing cycles. As shown in the **Fig. S7**, even after the 4th Cycle test, rGO-PDI-Co is functioning well in terms of H_2 production (Fig. S7). The decrease in the amount of hydrogen produced after 3rd cycle can be attributed to the degradation of PDI-Co under continious irradation ($\lambda > 400$ nm) and applied voltage (-0.4 V vs SHE) for >25 h. This is consistent with the previously reported Eosin Y/rGO/Pt,[9] Graphene-CNT/Fe_2O_3,[10] BiVO$_4$-rGO,[11] and Cu_2O-rGO/Pt [12]

References:

[1]   Huang, N. M.; Lim, H. N.; Chia, C. H.; Yarmo, M. A.; Muhamad, M. R.; Simple Room-Temperature Preparation Of High-Yield Large-Area Graphene Oxide. *Int J Nanomedicine.* **2011**; 6: 3443–3448.

[2]   Keerthi, A.; Valiyaveettil,   S.;   Regioisomers of Perylenediimide: Synthesis, Photophysical, and Electrochemical Properties. *J. Phy. Chem. B* **2012**, 116, 4603-4614

[3]   Atria, A. M.; Cortes, P.; Garland, M. T.; Baggio, R.; Two Isomorphous Imidazole (Him) Complexes: $[Mcl_2(Him)_2(H_2O)_2]$ (M = Co And Ni)   *Acta Cryst.* **2003**, 59, m396-m398.

[4].   Su, C.; Acik, M.; Takai, K.; Lu, J.; Hao, S.-j.; Zheng, Y.; Wu, P.; Bao, Q.; Enoki, T.; Chabal, Y. J.; Loh, K. P.; Probing The Catalytic Activity Of Porous Graphene Oxide And The Origin Of This Behaviour. *Nat Commun* **2012**, 3, 1298.

[5]   Ng, Y. H.; Iwase, A.; Kudo, A.; Amal, R.; Reducing Graphene Oxide on a Visible-Light BiVO4 Photocatalyst for an Enhanced Photoelectrochemical Water Splitting. *J. Phy. Chem. Lett.* **2010**, 1, 2607-2612

[6]   de Navarro, C. U.; Machado, F.; López, M.; Maspero, D.; Perez-Pariente, J. A SEM/EDX Study Of The Cobalt Distribution In Coapo-Type Materials. *Zeolites* **1995**, 15, 157-163.

[7].   Andreiadis, E. S.; Jacques, P.-A.; Tran, P. D.; Leyris, A.; Chavarot-Kerlidou, M.; Jousselme, B.; Matheron, M.; Pécaut, J.; Palacin, S.; Fontecave, M.; Artero, V.

Molecular Engineering Of A Cobalt-Based Electrocatalytic Nanomaterial For H2 Evolution Under Fully Aqueous Conditions. *Nat Chem* **2013**, 5, 48-53.

[8]   Polavarapu, L.; Xu, Q. H.; A Simple Method For Large Scale Synthesis Of Highly Monodisperse Gold Nanoparticles At Room Temperature And Their Electron Relaxation Properties. *Nanotechnology*, **2009**, 20,185606.

[9].   Mou, Z., Dong, Y., Li, S., Du, Y., Wang, X., Yang, P., Wang, S. Eosin Y Functionalized Graphene For Photocatalytic Hydrogen Production From Water. *Int. J. Hydrogen Energy* **2011**, 36, 8885-8893.

[10]   Young Kim, J., Jang, J.-W., Hyun Youn, D., Yul Kim, J., Sun Kim, E., Sung Lee, J. Graphene–Carbon Nanotube Composite As An Effective Conducting Scaffold To Enhance The Photoelectrochemical Water Oxidation Activity Of A Hematite Film. *RSC Advances* **2012**, 2, 9415-9422.

[11]   Ng, Y. H., Iwase, A., Kudo, A., Amal, R. Reducing Graphene Oxide On A Visible-Light Bivo4 Photocatalyst for an Enhanced Photoelectrochemical Water Splitting. *J. Phy. Chem. Lett.* **2010**, 1, 2607-2612.

[12]   Tran, P. D., Batabyal, S. K., Pramana, S. S., Barber, J., Wong, L. H., Loo, S. C. J., A Cuprous Oxide–Reduced Graphene Oxide (Cu2O–rGO) Composite Photocatalyst for Hydrogen Generation: Employing rGO as an Electron Acceptor to Enhance the Photocatalytic Activity and Stability of Cu2O. *Nanoscale*, **2012**, 4, 3875-3878.

Appendix I

MALDI-TOF spectrum of **PDI**